From Emergence to Eruption: Data-Driven Modeling of Solar Active Regions

Mark Cheung
Lockheed Martin Solar & Astrophysics Laboratory, Palo Alto, CA

Coupling & Dynamics of the Solar Atmosphere, IUCAA, Pune, India, Nov 10th-14th 2014

- Challenges and opportunities
- Data-inspired, data-constrained and data-driven models
- Application of data-driven modeling for
  - NOAA AR 11158
  - Homologous helical jets observed by SDO, Hinode and IRIS
- Concluding remarks

Challenges

- Without routine measurements of the vector ***B*** in the corona (and until recently, the chromosphere), how do we obtain 3D magnetic models of active regions (ARs)?
- How do we capture the evolution of ARs over the course of hours or even days (free energy accumulation timescale)?
- How do we apply the lessons learned from idealized MHD models (dealing with simplified physics and/or magnetic configurations) to real ARs on the Sun?
- How do we meld together improvements in observational capability and theory to advance our understanding of AR evolution and associated dynamic phenomena?

Opportunities

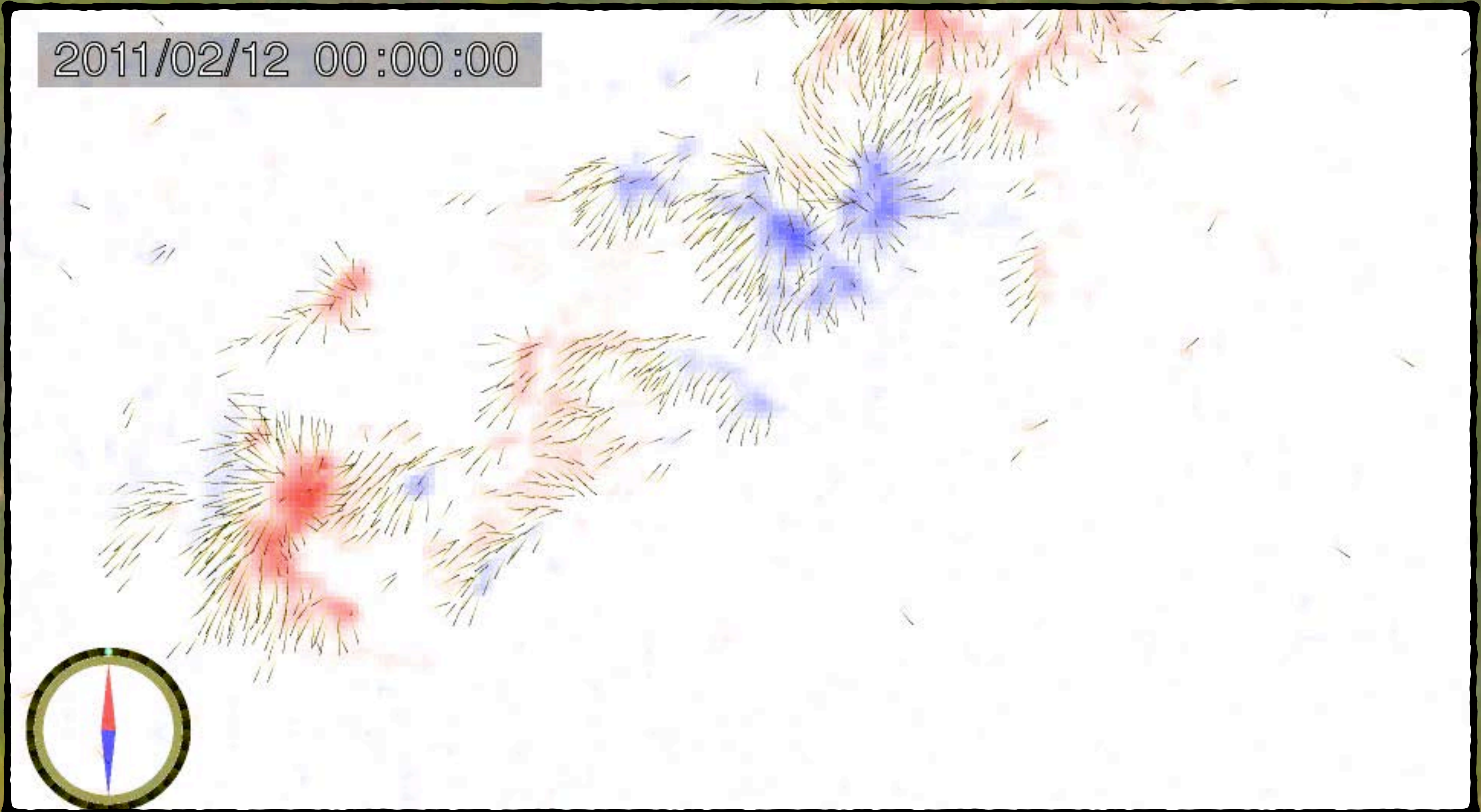

With easy access to data, any modeler can be an armchair observer. How do we exploit the opportunities made available by long observational sequences from space missions?

Opportunities: Data + Modeling

- Data-inspired Models: Simplified setups to mimic observed scenarios
- Data-Constrained Models: Time-independent models satisfying observations at an instant in time
- Data-Driven Models: Time-dependent models evolved using Faraday's law with time-dependent bottom boundary conditions set by observational data.

Examples of Data-inspired Models

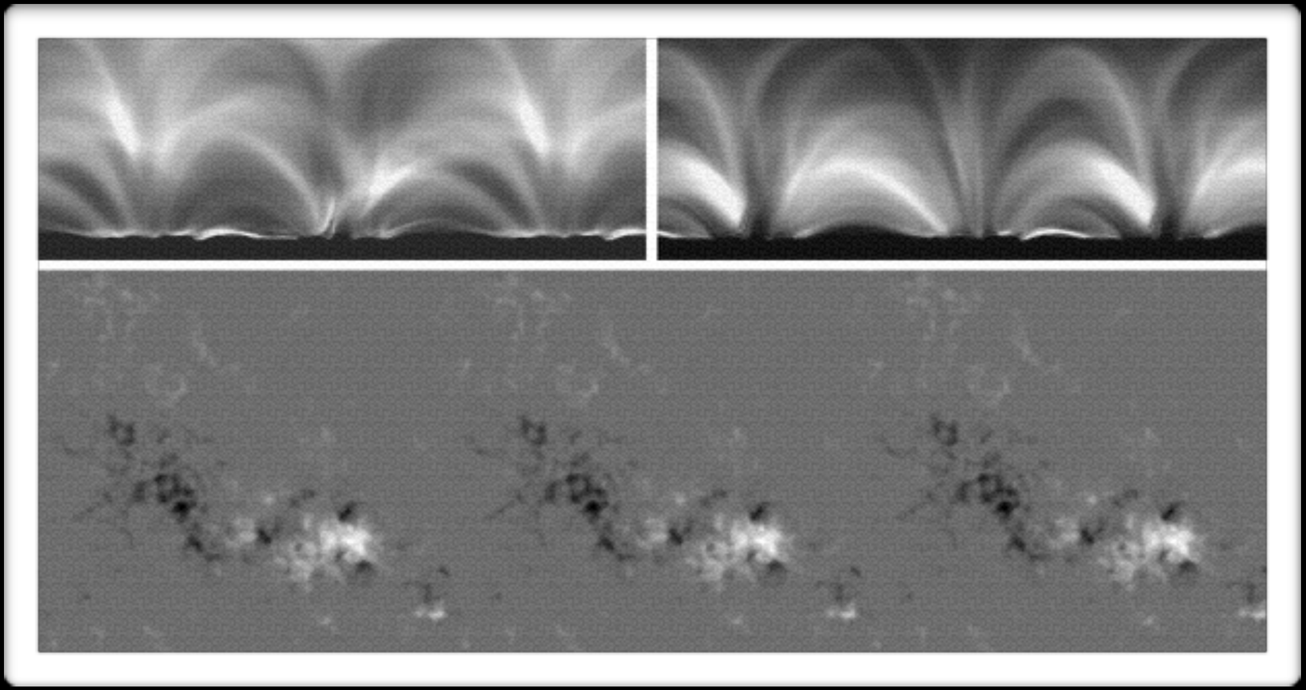

Left: Gudiksen & Nordlund (2004, ApJ)

- Downscaled MDI magnetogram of an AR by a factor of 4.
- Initial condition is a potential field.
- Bottom boundary evolved by horizontal flows with statistical properties mimicking solar surface evolution.

Right: Fan (2011, ApJ)

- Smoothed MDI magnetogram of AR 10930 so that B=3 kG -> 200 G.
- A twisted flux rope was emerged into the pre-existing sunspot. The interaction between the two magnetic systems leads to a coronal mass ejection.

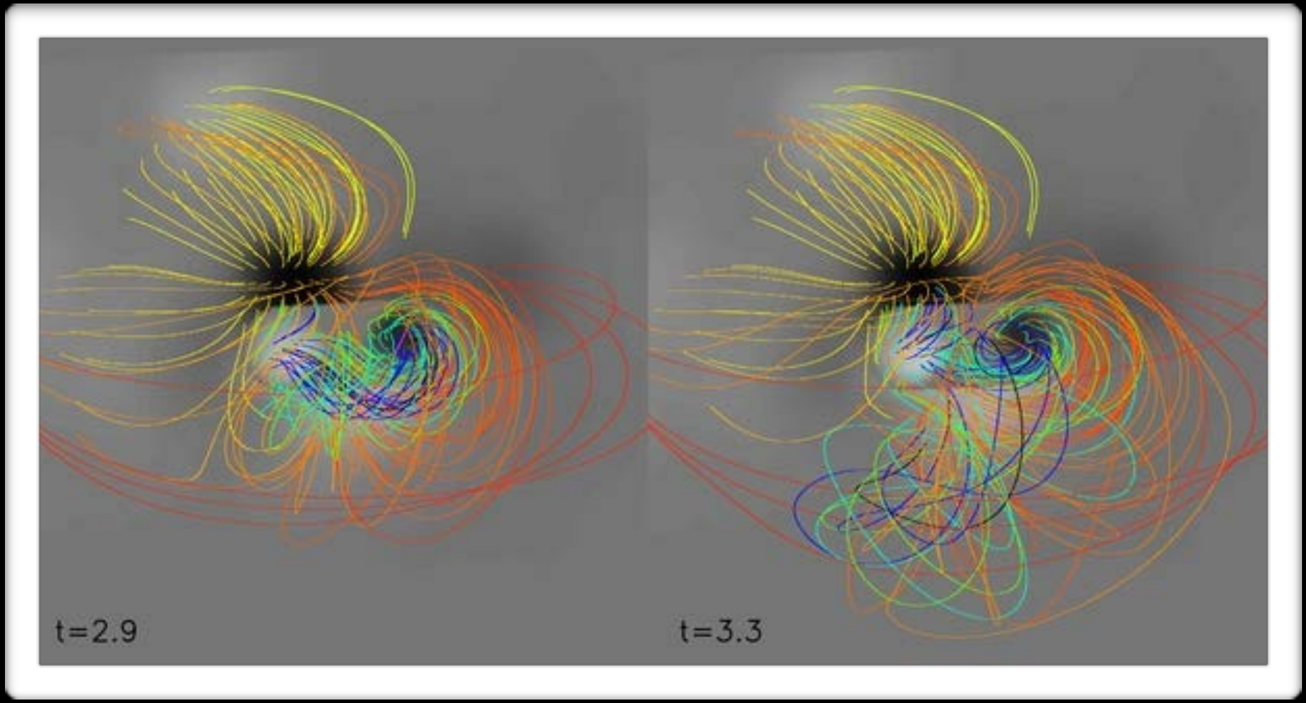

Examples of Data-Constrained Models

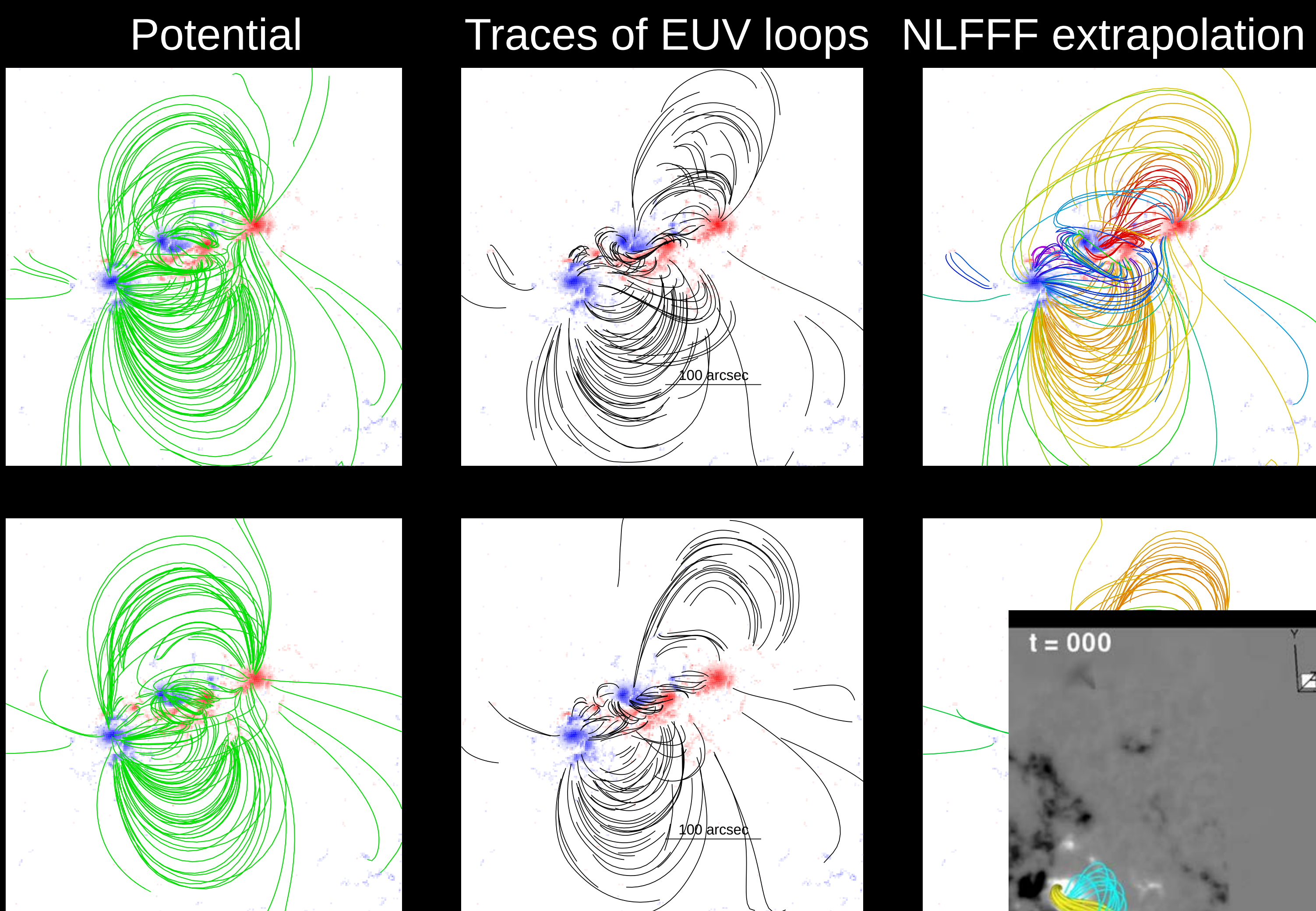

Left: Malanushenko et al. (2014): Use line-of-sight B and EUV loops to constrain NLFFF field (as opposed to using vector magnetograms).

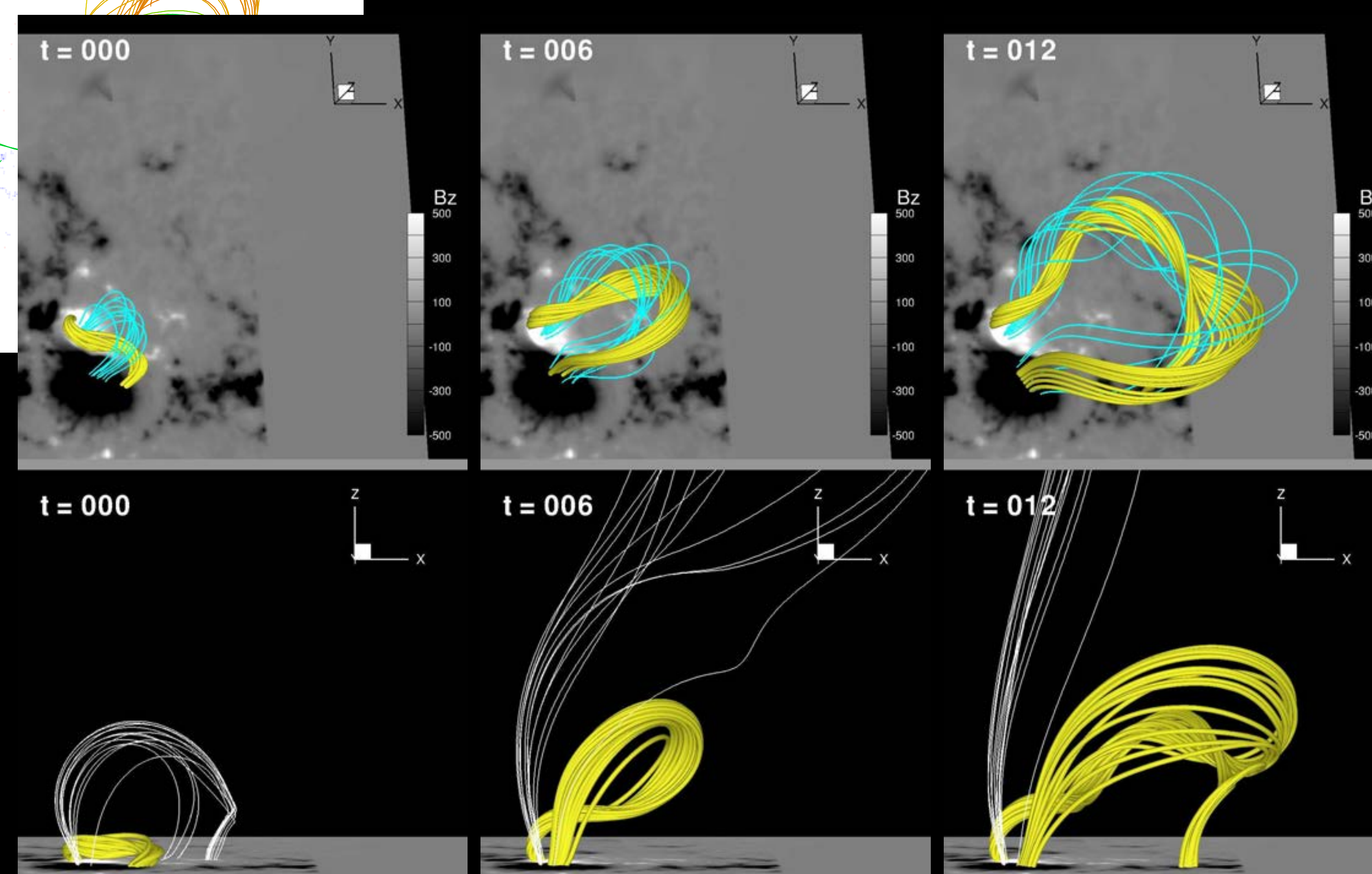

Right: Jiang et al. (2013): Use vector magnetogram for NLFFF extrapolation, then feed the model field into an MHD code. This leads to an eruption. NB: The vector B at the bottom boundary is fixed in time in the MHD model.

Examples of Data-Constrained Models

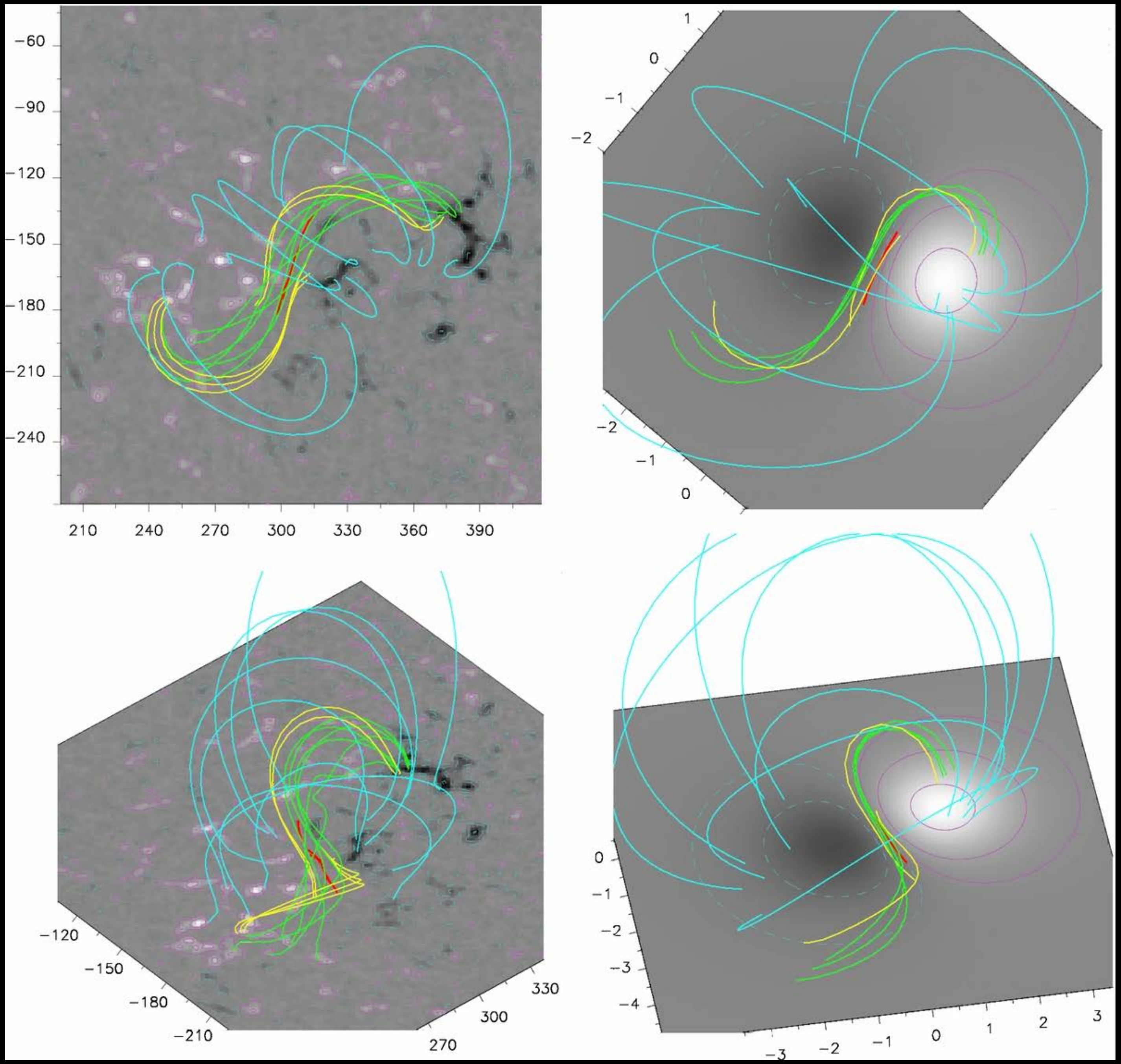

Flux rope insertion (data-constrained magnetofrictional model)

MHD model (data-inspired)

Savcheva et al. (2012): Comparison of sigmoid models shows consistent magnetic topologies between NLFFF and MHD models of sigmoids.

Data-Driven Models

- Van Ballegooijen, Priest & Mackay (2000)
  - Solve induction equation with velocity proportional to Lorentz force:
  - Yeates, Mackay & Van Ballegooijen (2008)
  - Global magnetofrictional model of coronal field in response to observed changes in photospheric field, including
    - Differential rotation, meridional circulation
    - Flux dispersal and cancellation
    - Appearance of AR-scale, twisted bipoles
  - Correctly reproduces filament chirality and location
  - Memory of corona ~ 6 weeks to a few months

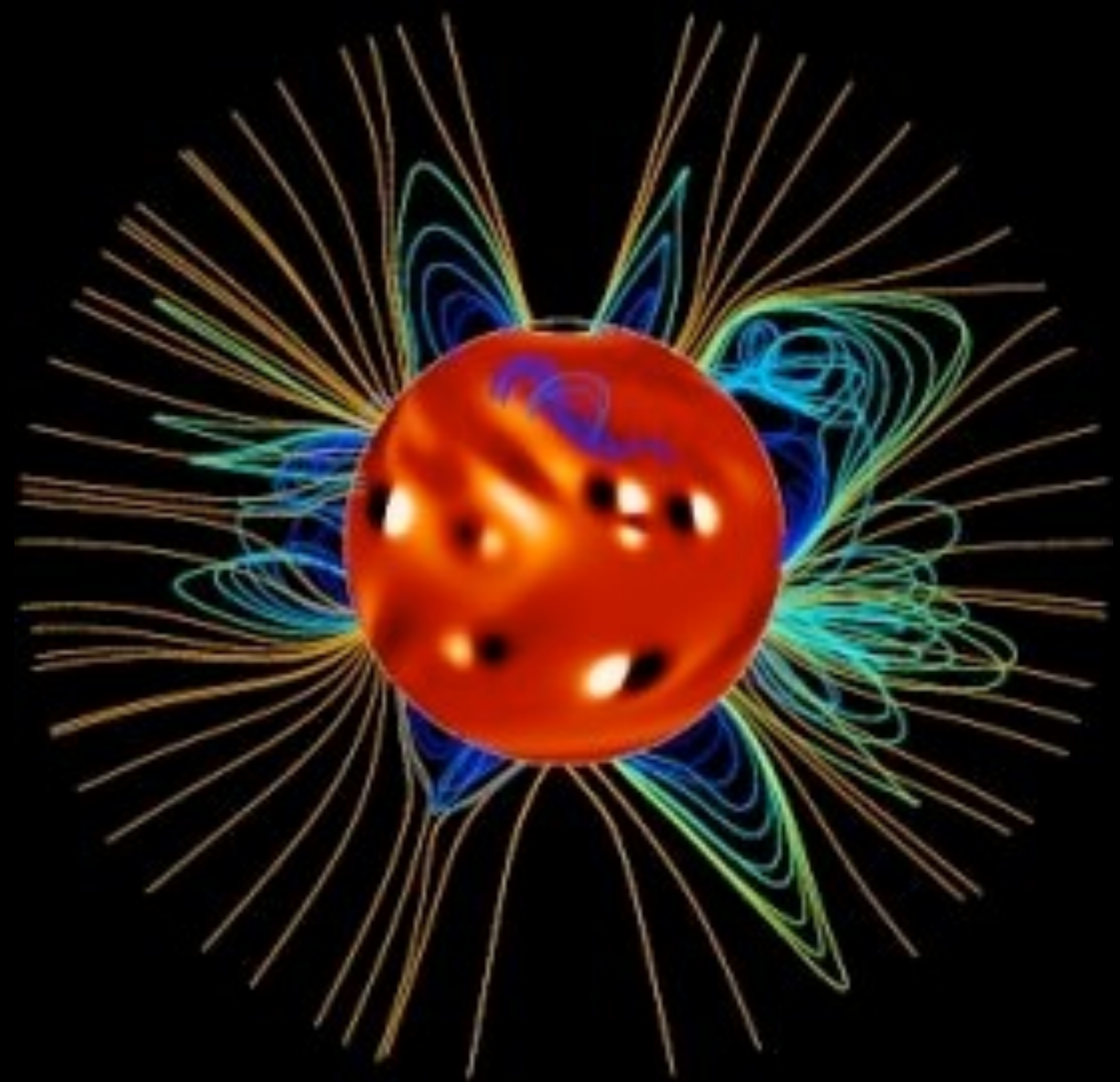

Yeates, Mackay & Van Ballegooijen 2008
See also Yeates 2013

Data-Driven Models of AR Evolution

- Gibb et al. (2014) used MDI magnetograms to drive a magnetofriction model to examine the evolution of AR 10977 over a seven-day period.
- The free energy stored in the model AR is sufficient to power the observed B1.4 flare.
- See talk by Chitta for application of this method to modeling the magnetic carpet.

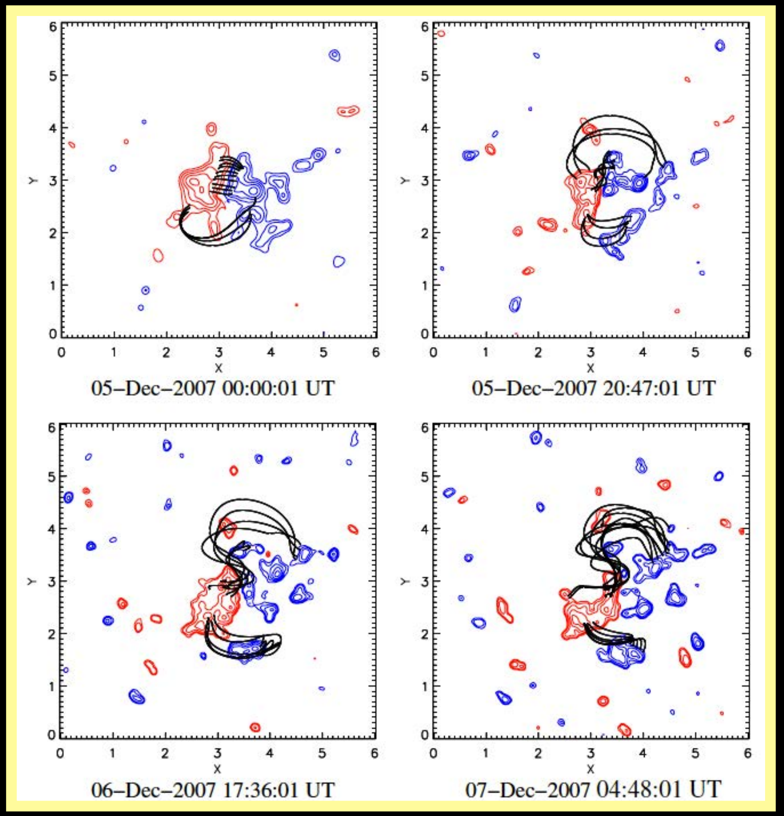

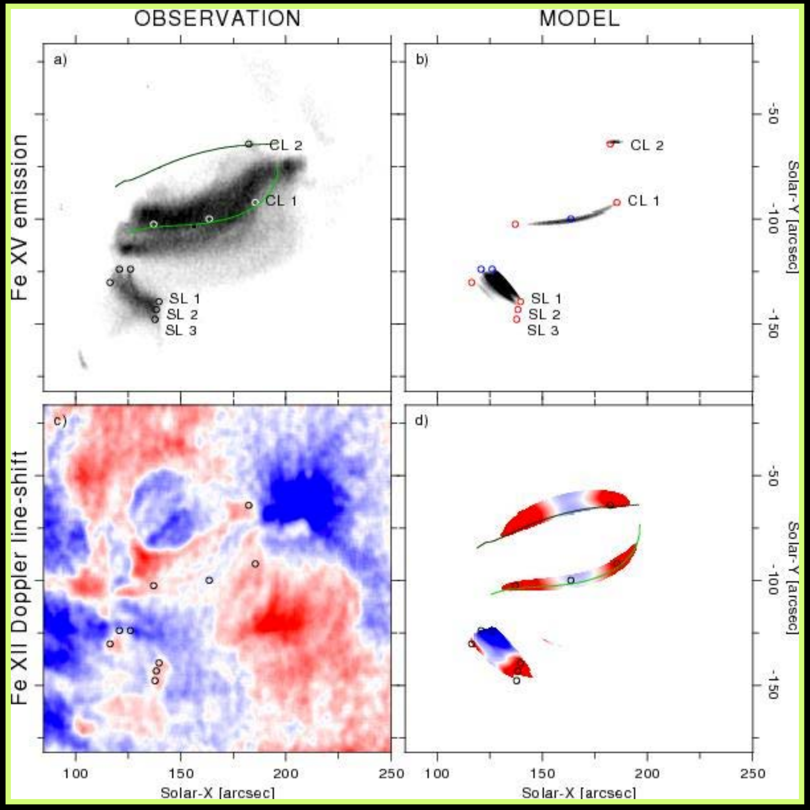

- Bourdin et al. (2013) used a sequence of Hinode NFI magnetograms to drive an MHD model of the evolution of an AR in its decay phase.
- They compared synthetic observables (e.g. EUV lines) with observations.

Magnetofriction

- Balance of Lorentz force and fictitious frictional force (Yang, Sturrock & Antiochos, 1986; Craig & Sneyd 1986)
  - Plasma velocity proportional to Lorentz force: $v = \nu^{-1}\, j \times B$ where ν is the frictional coefficient
  - Evolve magnetic field according to Induction Equation
- Total magnetic energy in volume monotonically decreasing (provided net Poynting flux through boundaries is zero).
- Valori, Kliem & Fuhrmann 2007 used magnetofriction for non-linear force-free field extrapolation using a single vector magnetogram.
- Our approach is fundamentally different from NLFFF extrapolation. Instead of a single magnetogram, we use temporal sequence of magnetograms to advance the model forward in time. This type of model has memory.

Data-Driven Models of AR Evolution

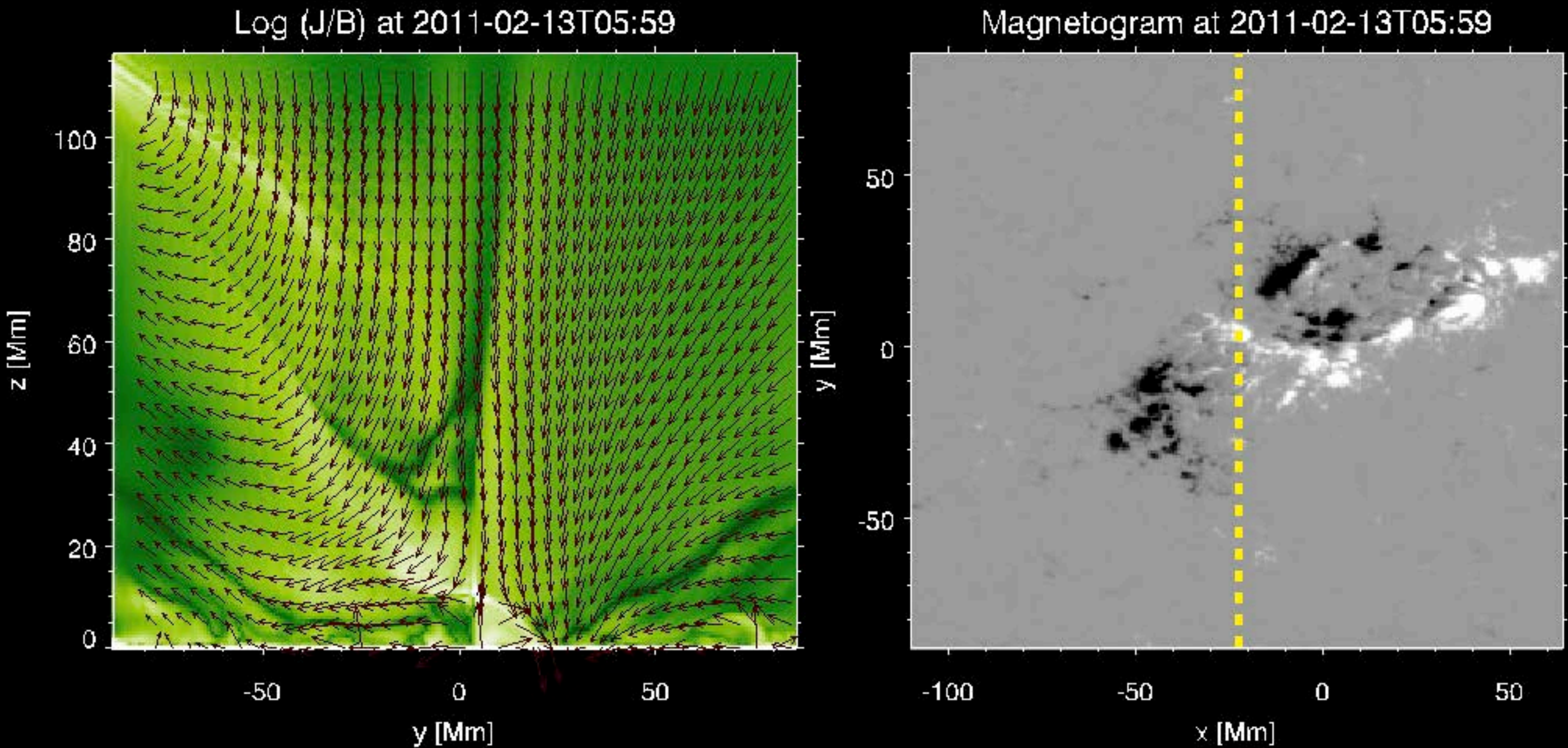

- Cheung & DeRosa (2012) use HMI magnetograms to model AR 11158. Sheared field results in (multiple) flux-rope ejections (cf. Mikic & Linker 1994; Antiochos, DeVore & Klimchuk 1998; Manchester et al 2004).

E-fields retrieved from HMI magnetograms

- Instead of using ad hoc assumptions about the electric field at the photosphere, the group at Space Sciences Lab, UC Berkeley developed a method to use the full vector magnetograms and Dopplergrams to constrain the photospheric electric field. Method described in Fisher, Welsch & Abbett (2012), and Kazachenko (2014, available on arxiv).
- The next slides show preliminary results from a data-driven model using electric field solutions from the Berkeley group.
- This work is done as part of the Community Global Evolutionary Model (CGEM) project funded by NSF and NASA. A spherical model is being developed as part of this project.

Steps Toward Vmag-Driven Simulations

"Research" grade

- Synthesize Coronal Loop Structures, Compare with Observations
- Drive Evolutionary Coronal Field Model
- Retrieve Photospheric Electric Field
- Resolve 180 degree ambiguity
- Stokes inversion → Vector Magnetic Field
- Polarized Filtergram Measurements

Magnetograms at different heights

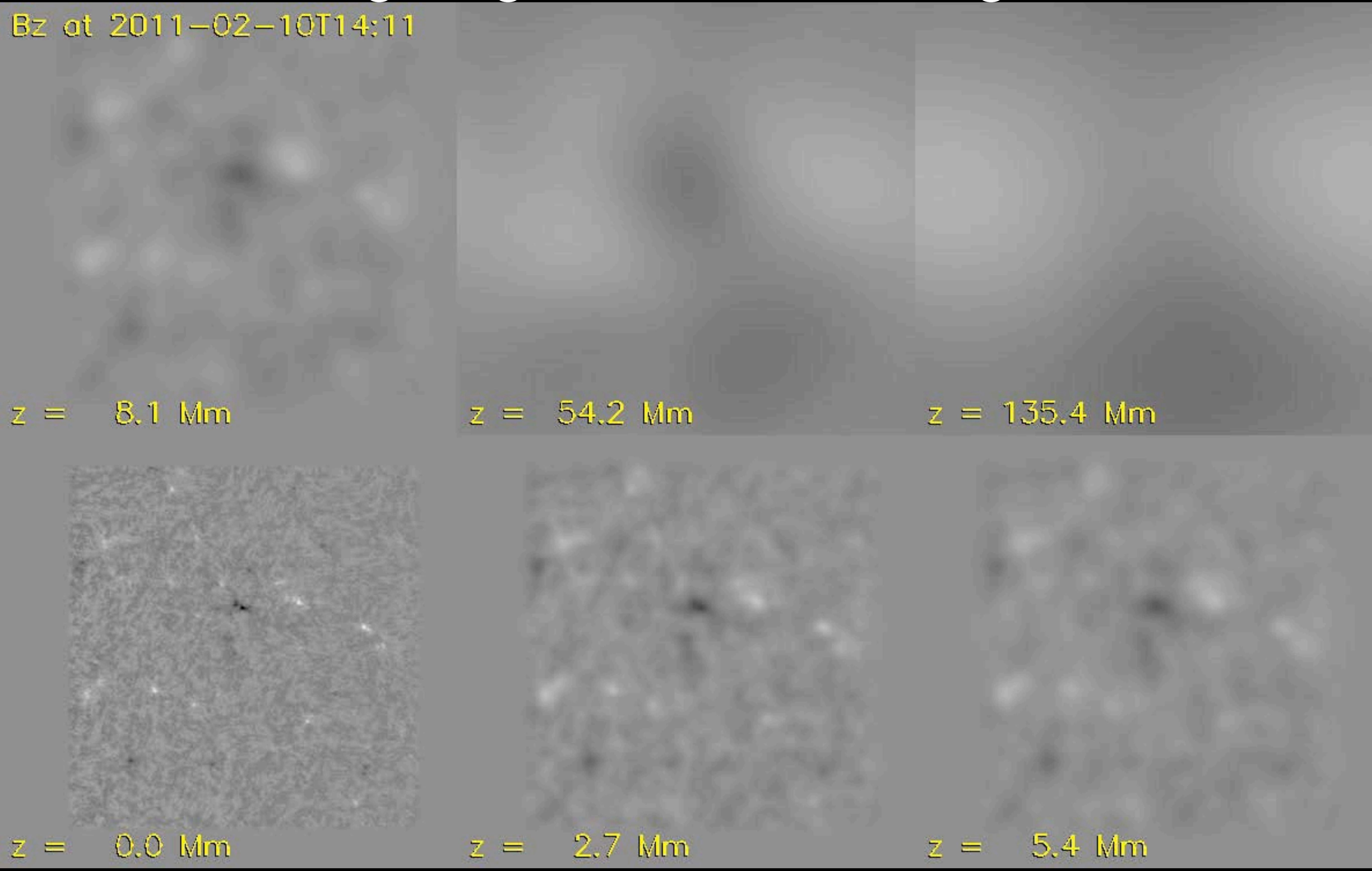

Visualization of Field Lines

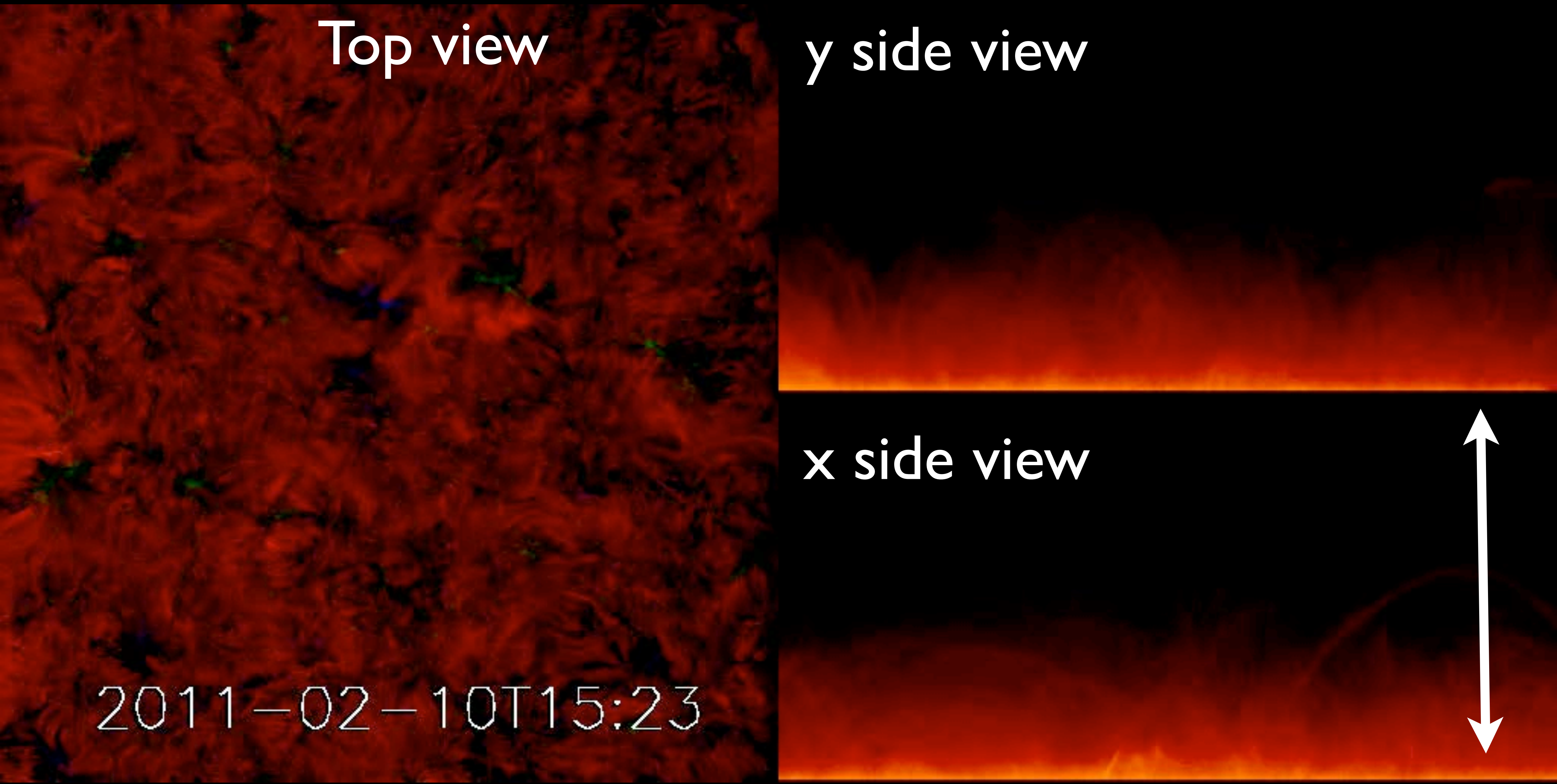

Only the lowest 66 Mm shown: Not one-to-one aspect ratio.

Orange ~ $\int_{los} \langle j^2 \rangle dl$, *where* $\langle j^2 \rangle$ *is fieldline-averaged* j^2

Positive polarity B_r

Negative polarity B_r

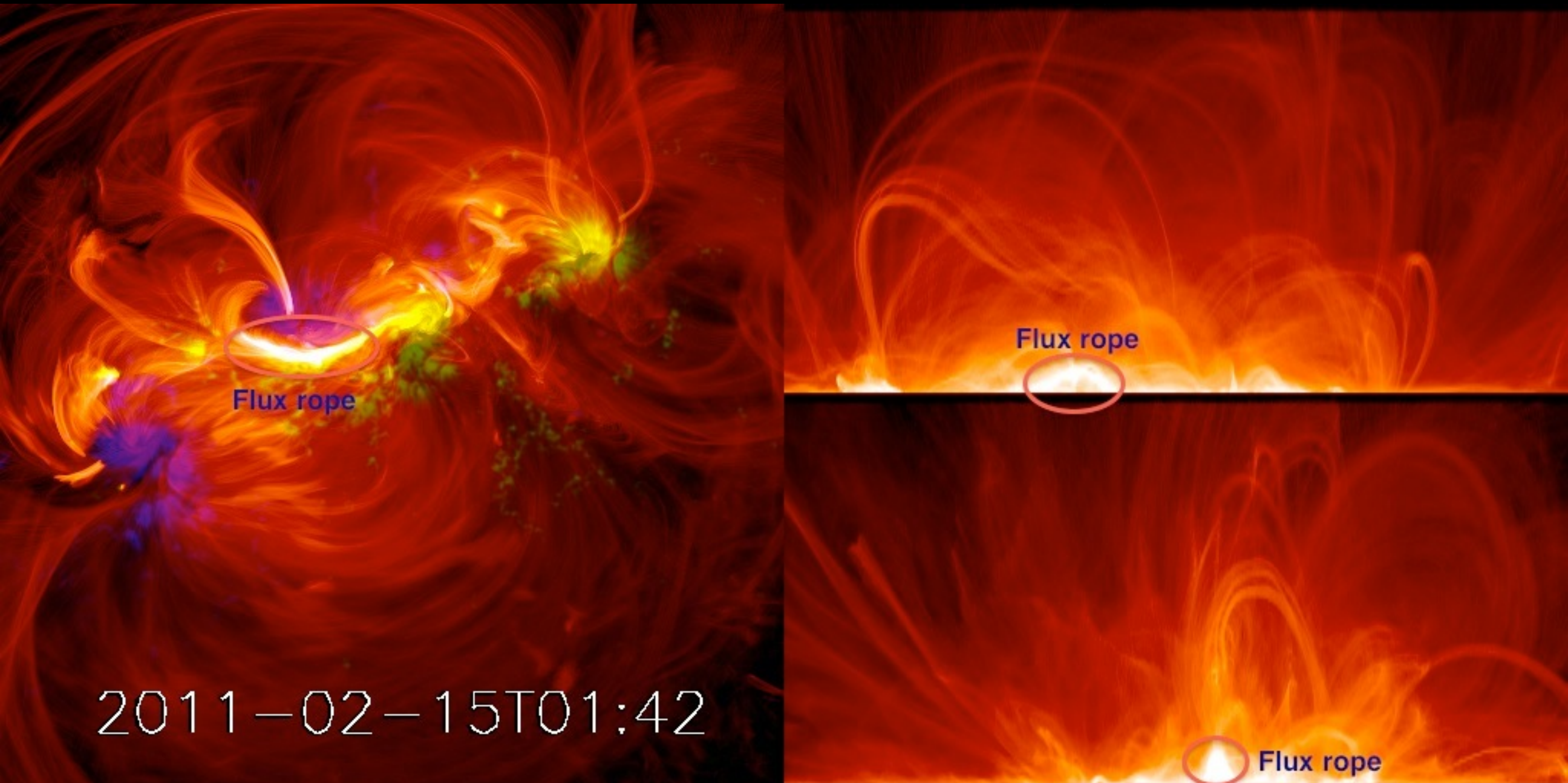

- There is no impulsive eruption at the time of the observed X-flare. However, moments before this time, a current-carrying flux rope is observed to form and is eventually ejected, though the rise time is on the order of hours.
- An extension of this work is to use the destabilized configuration as the initial condition for an MHD simulation.

Modeling of Homologous Helical Jets

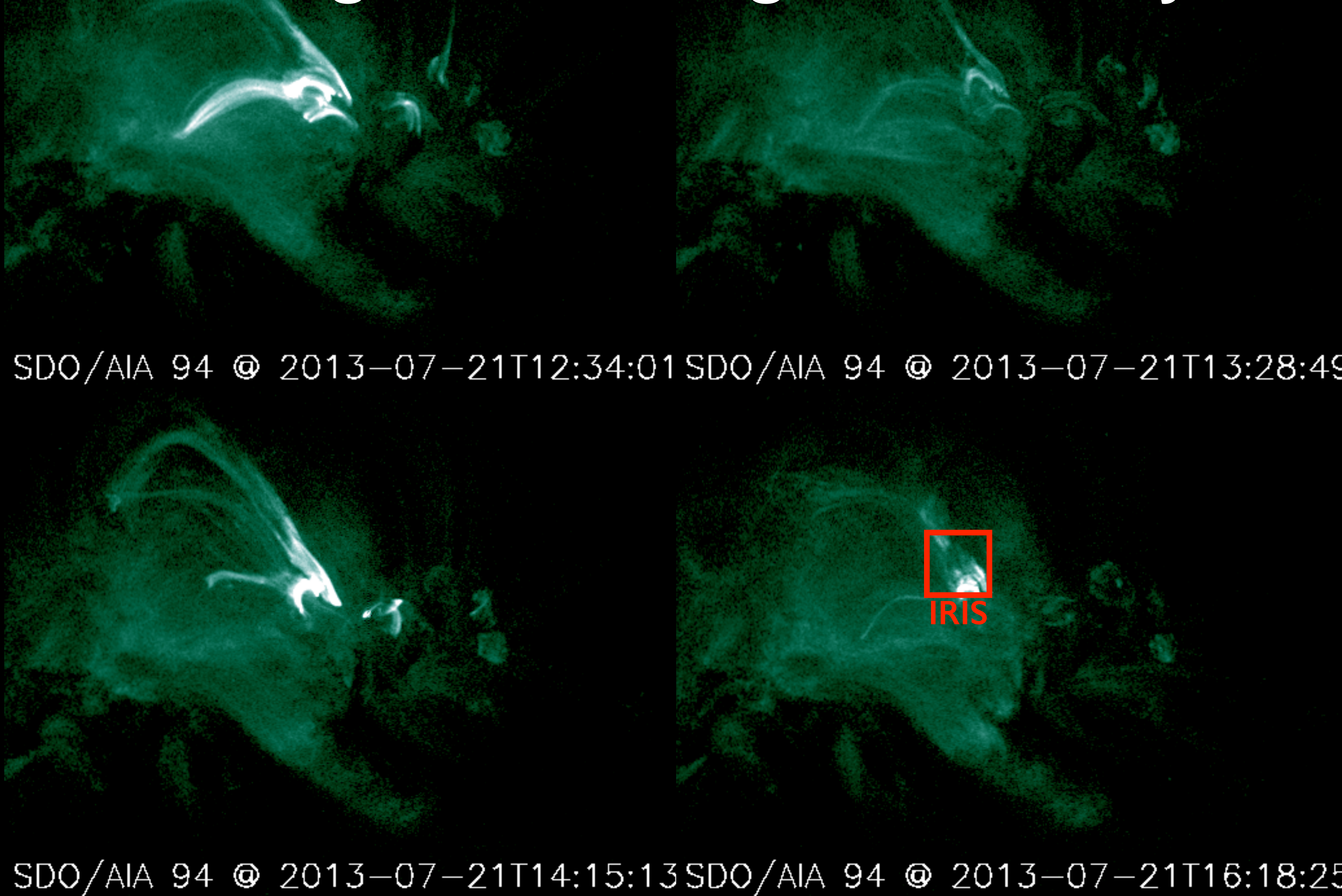

`

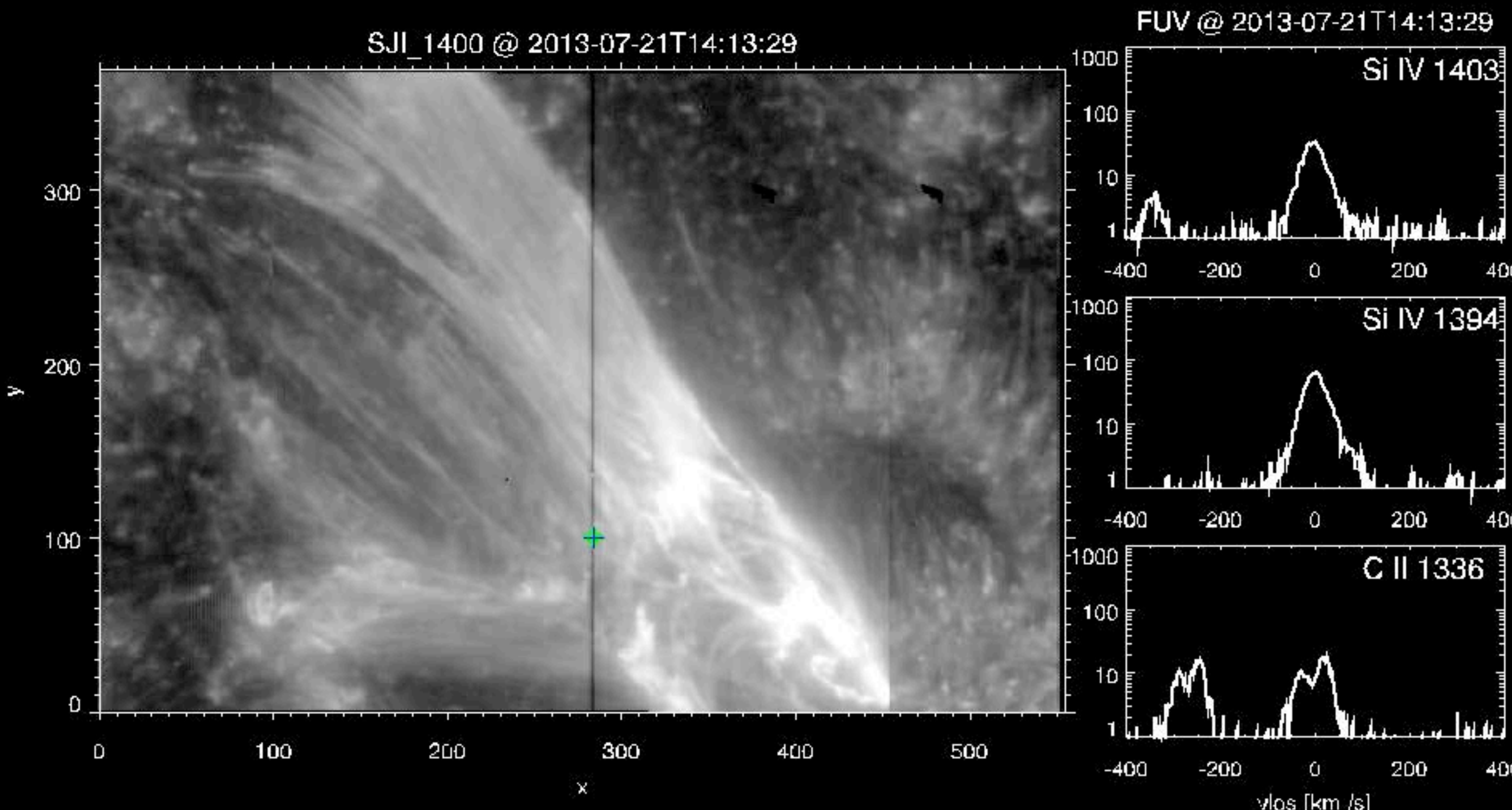

- SJI 1400, SJI 1330 and SJI 2796 @ 24s cadence, 60” x 60” FOV, 0.167” arcsec pixel size
- 20-step NUV and FUV spectral rasters with 2 arcsec steps, 2 min / raster, 38” x 60” FOV

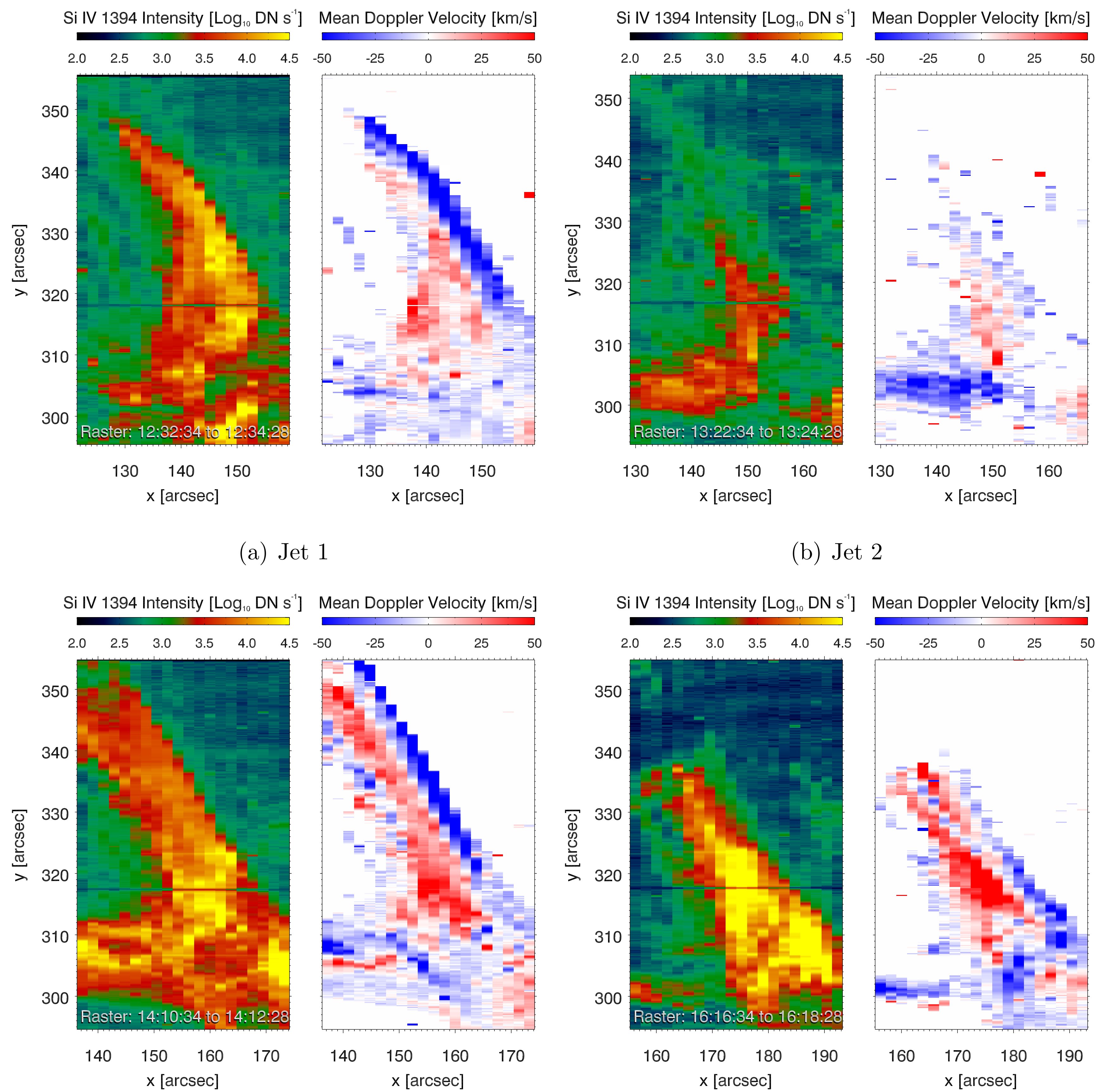

(a) Jet 1 (b) Jet 2 (c) Jet 3 (d) Jet 4

Doppler shift maps using the Si IV 1394 line (log T = 4.8) observed by IRIS shows helical motion in all four jets (Cheung et al, submitted).

Similar pattern reported by Pike & Mason (1998) using a TR line observed by SoHO/CDS.

Models of Jet Formation

- Heyvaerts & Priest (1977): Reconnection between emerging flux and ambient field for solar flares.

- MHD models of jet formation due to interaction of emerging flux with ambient coronal field. See Yokoyama & Shibata 1995; Miyagoshi & Yokoyama 2004; Archontis et al. 2005; Galsgaard et al. 2005; Isobe et al. 2007; Moreno-Insertis et al. 2008; Nishizuka et al. 2008; Heggland et al. 2009; Archontis et al. 2010; Archontis & Hood 2013; Moreno-Insertis & Galsgaard 2013; Takasao et al. 2013; Fang et al. 2014.

- Pariat, Antiochos & DeVore (2010) showed that persistent twisting of a parasitic polarity embedded in opposite field region can lead to recurrent, homologous jets. In each episode, a helical jet is emitted after twisting the field by N~1 winding (exact value depends on geometry).

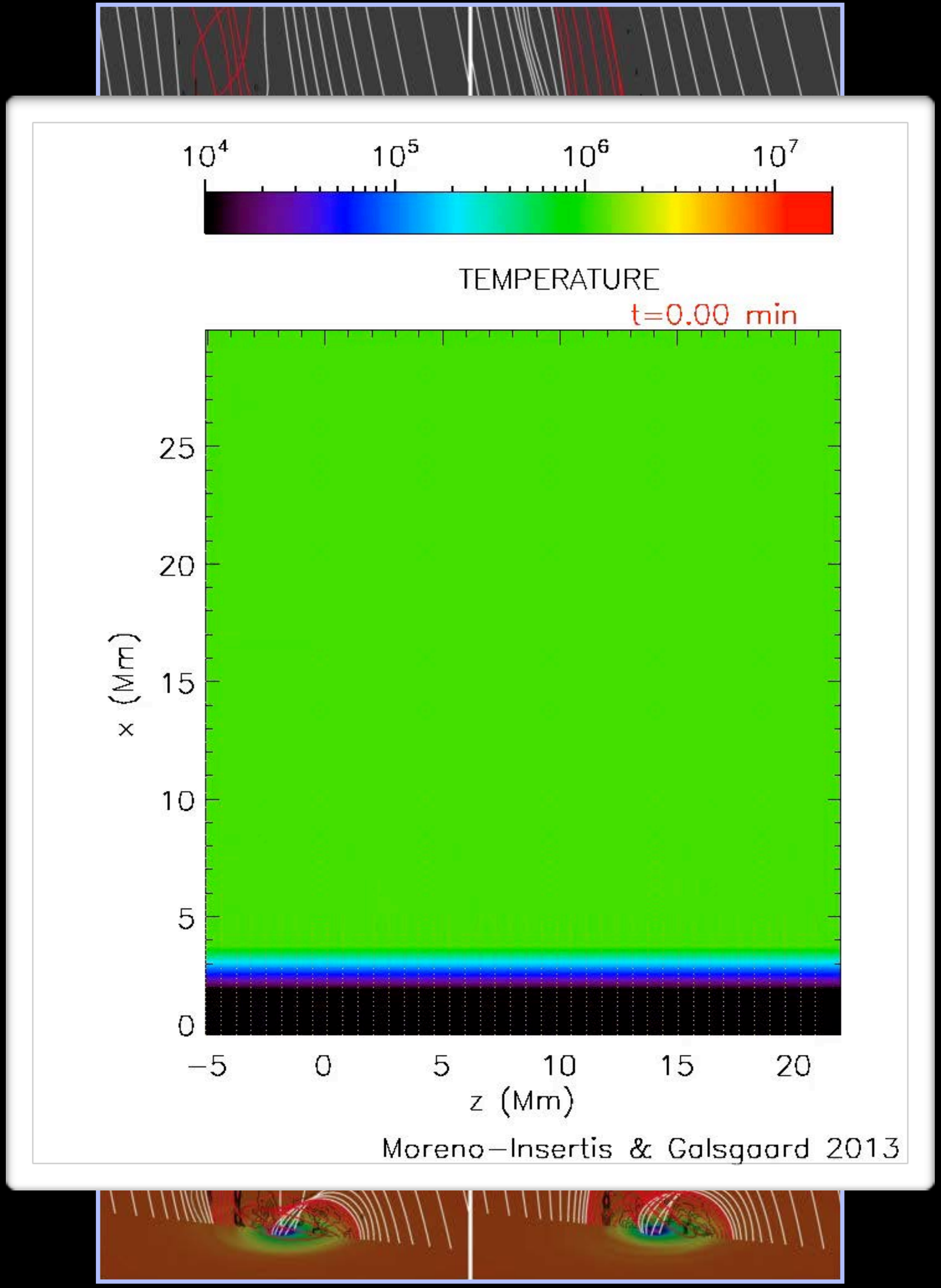

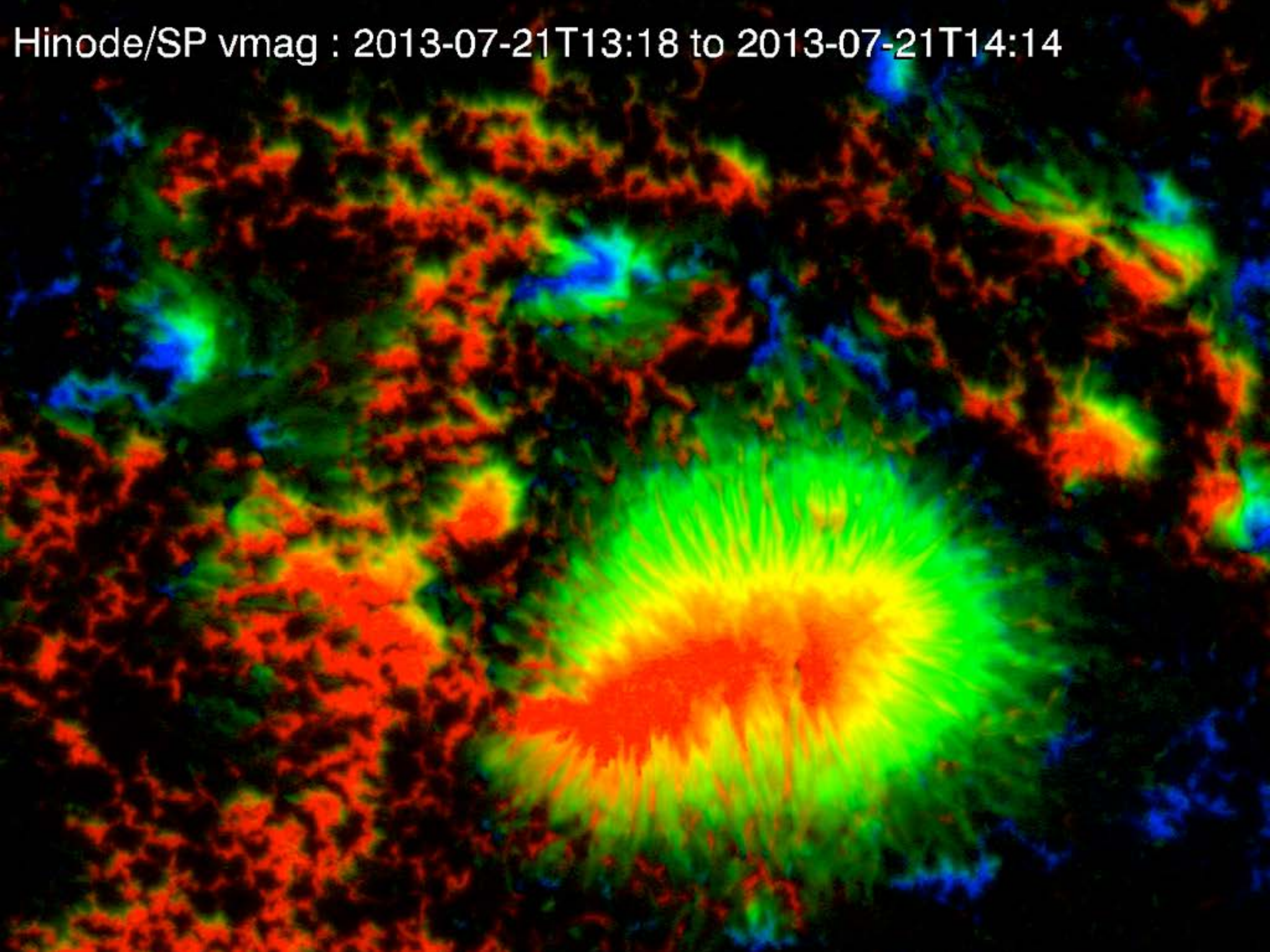
Hinode/SP vmag : 2013-07-21T13:18 to 2013-07-21T14:14

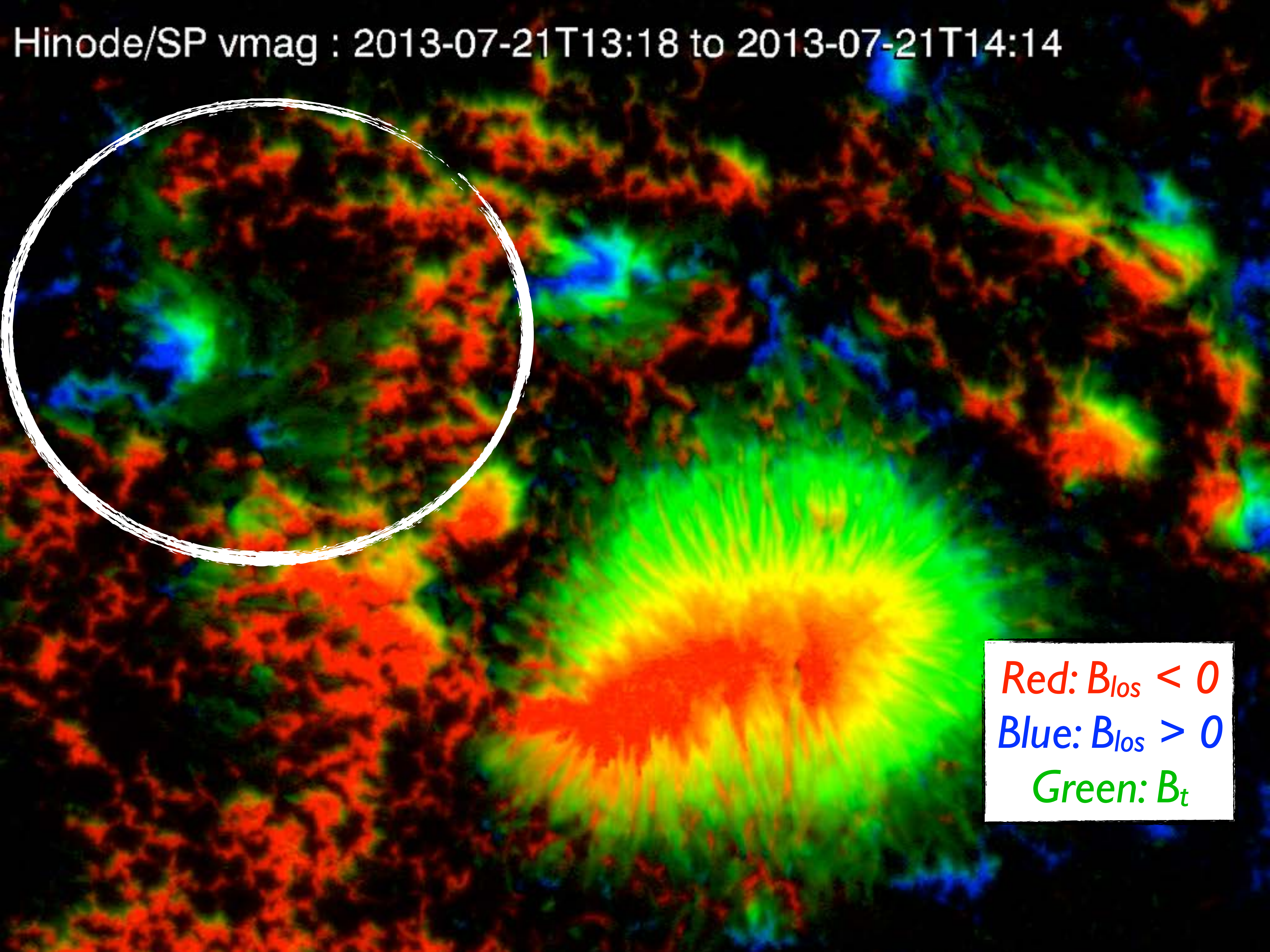
Hinode/SP vmag : 2013-07-21T13:18 to 2013-07-21T14:14
Red: $B_{los} < 0$
Blue: $B_{los} > 0$
Green: B_t

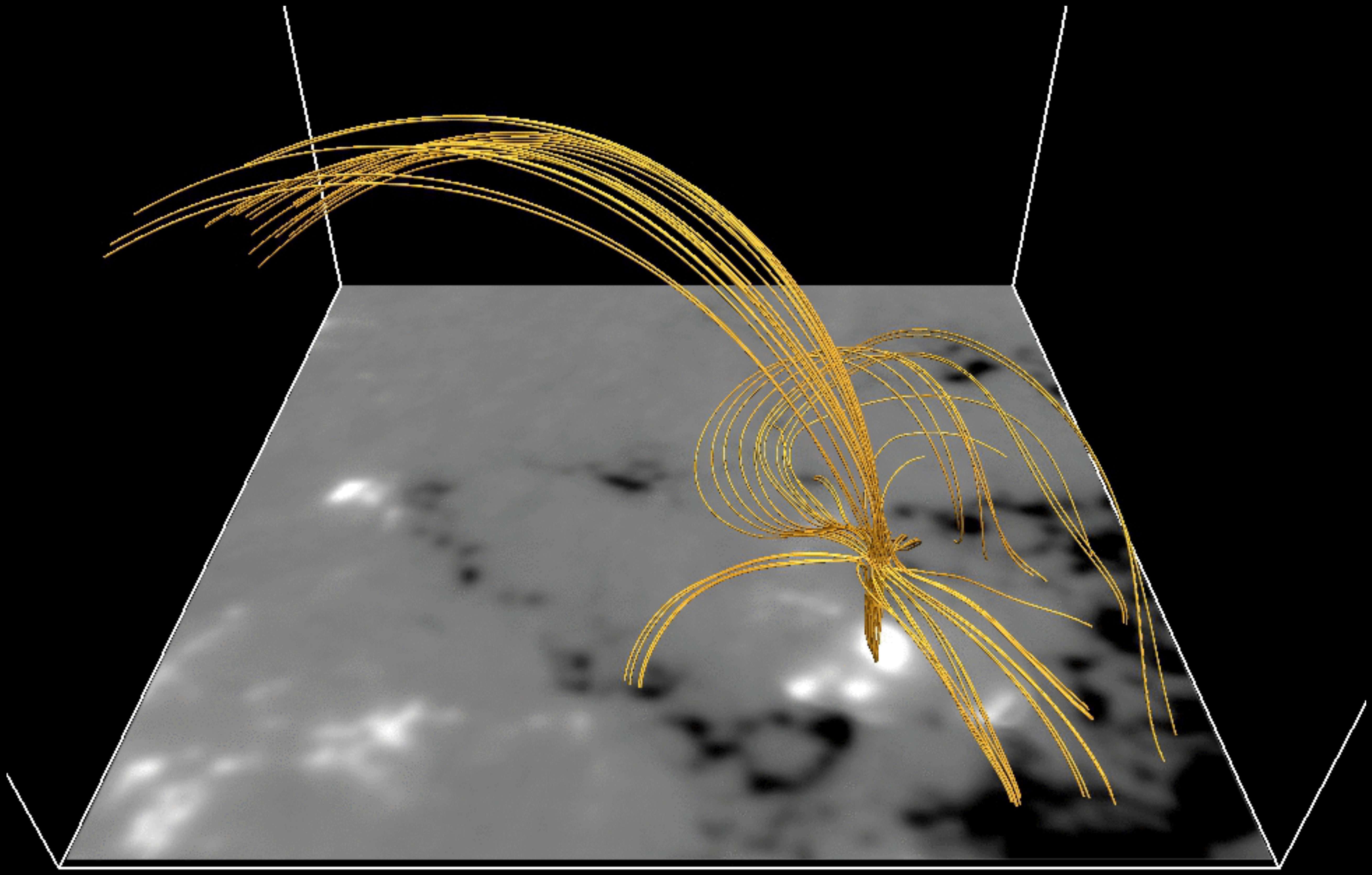

The parasitic pore + network field give a fan-spine topology for the overlying chromospheric/coronal magnetic field (see also Masson et al. 2009).

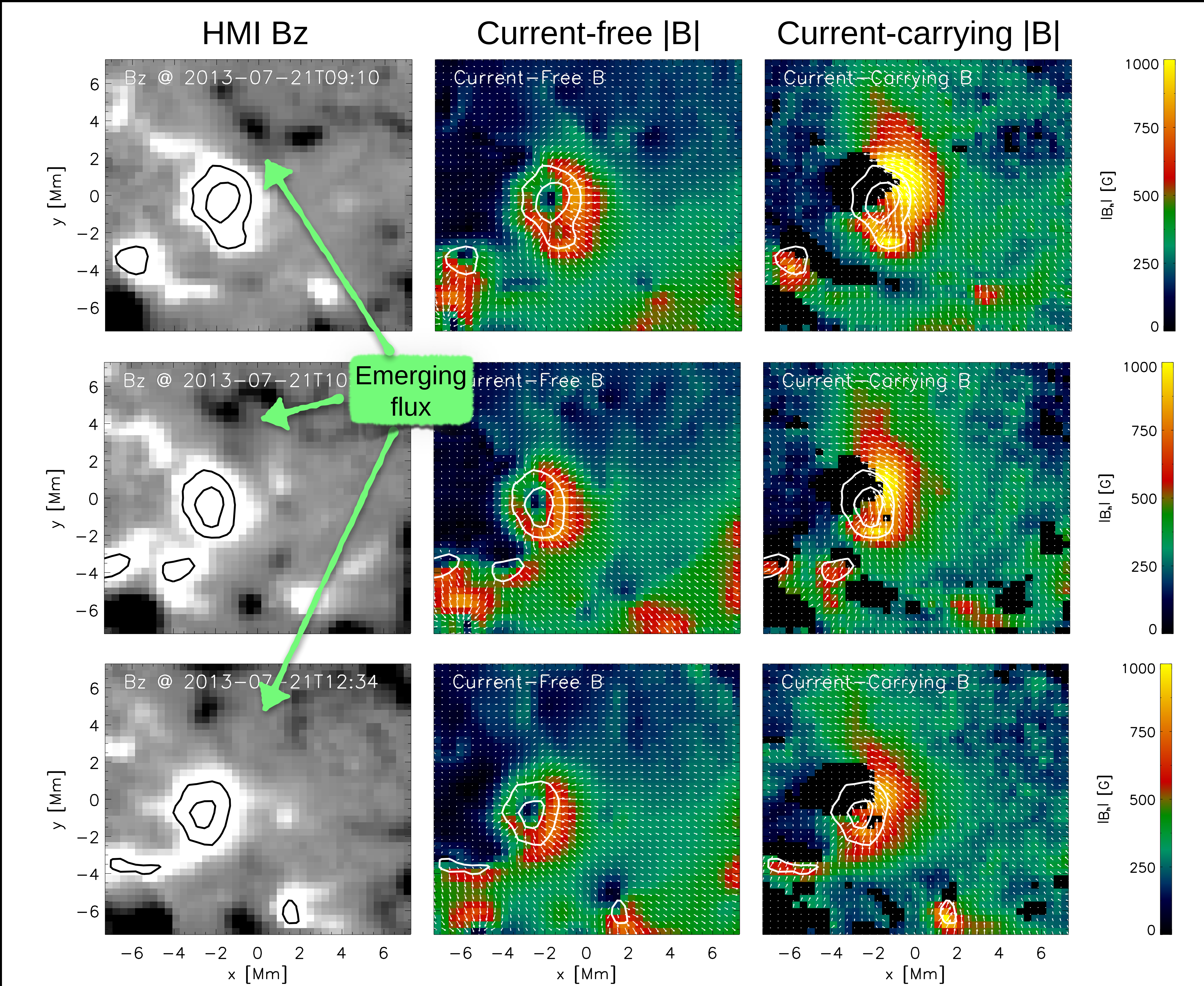

HMI Bz
Current-free |B|
Current-carrying |B|
Bz @ 2013-07-21T09:10
Current-Free B
Current-Carrying B
Emerging flux
Bz @ 2013-07-21T12:34
y [Mm]
x [Mm]
|B_h| [G]

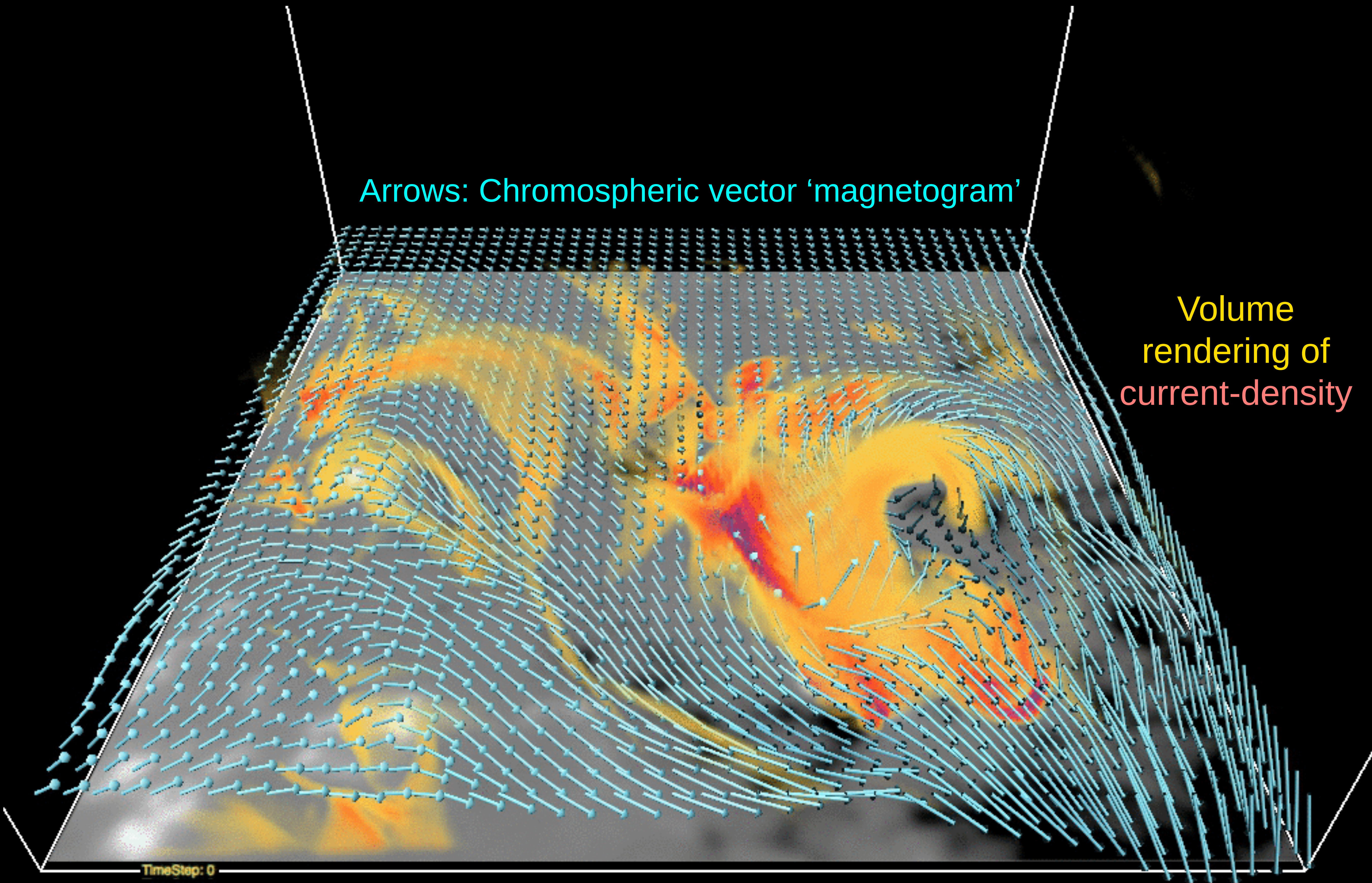

Magnetofriction model of homologous helical jets driven by HMI vector magnetograms (Cheung et al., submitted).

In a nutshell, the data and model support the mechanism proposed by Pariat et al. (2009, 2010) for homologous jets.

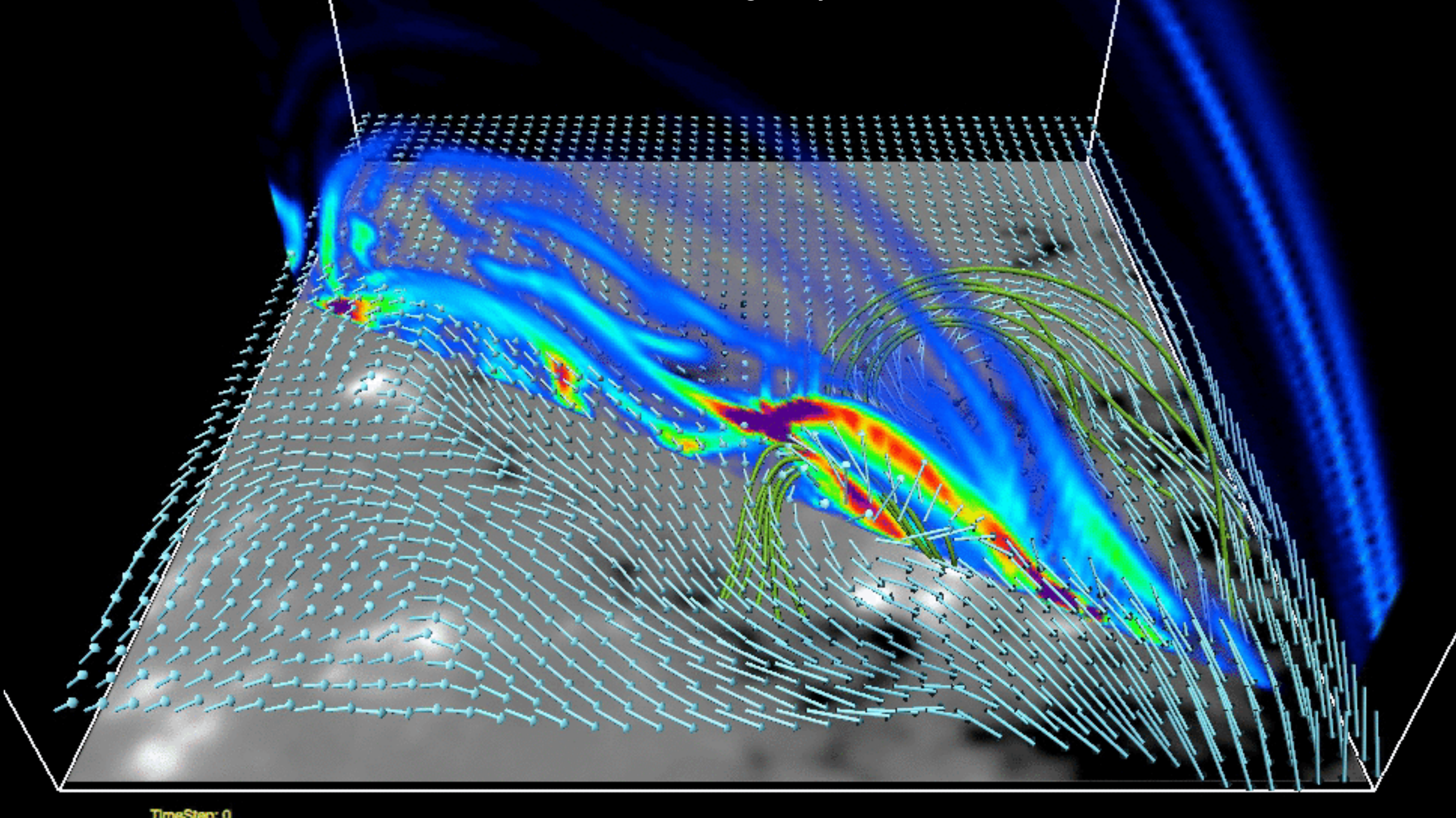

Magnetofriction model of homologous helical jets driven by HMI vector magnetograms (Cheung et al., submitted).

Concluding remarks

- High-cadence vector magnetograms from SDO/HMI is opening the door to a time-dependent, data-driven approach to modeling how coronal fields evolve in response to photospheric driving.
- Data-inspired, data-constrained and data-driven modeling ties together recent developments in numerical models and observational capability.
    - Modelers can go beyond making statements such as: *"If the Sun were to produce a symmetric, idealized flux rope satisfying the Titov-Demoulin model, it would erupt this way."*
    - Observers can back up statements like: *"The flux cancellation events are likely the cause of these jets."*
- This area of research is still in its infancy. This line of research needs to be pursued much further before becoming mature.
- Researchers should seize the opportunities and tackle the challenges.